Ingeniería y Competitividad
Vol 27 (1) 2025 doi: 10.25100/iyc.v27i1.14807

Vol 27 (1)

ISSN
0123-3033
e- 2027-8284

Original Article

Economic evaluation of Cu-impregnated manganese for CO2 capture in combustion with solid oxygen carriers

Evaluación económica de manganeso impregnado con Cu para captura de CO2 en combustión con transportadores sólidos de oxígeno

Carmen R. Forero[1] Eduardo Arango Durango[1] Francisco J. Velasco[1] Sandra E. Peña[2]

[1] Universidad del Valle, Eidenar, Cali, Colombia.
[2]Universidad de Guayaquil, Guayaquil, Ecuador.

Abstract

Introduction: Chemical Looping Combustion (CLC) is a promising technology for CO2 capture.
Objective:this study aimed to evaluate Cu-impregnated manganese ore (OXMN009P) as an effective oxygen carrier for this process, specifically using CO and H2 as fuels.
Methodology: the methodology involved thermogravimetric analysis (TGA) and batch fluidized bed reactor (bFB) testing to assess the material's performance.
Results: he results showed that OXMN009P exhibited a reaction rate index (RI) ranging from 6.1 to 20.1% /min. It also achieved high fuel conversion efficiencies, nearly 100% for H2 and approximately 70% for CO, demonstrating improved reactivity and oxygen transport capacity. Furthermore, the particle lifetime was extended to 2031 hours, significantly reducing the need for annual solids inventory replenishments.
Conclusions: in conclusion, the economic analysis suggests that the material cost of OXMN009P would not be a limiting factor for the implementation of CLC technology.

Keywords: Chemical looping combustion, Manganese ore, Copper impregnation, Rate index, Particles lifetime.

Resumen

Introducción: la combustión con transportadores sólidos de oxígeno (CLC por sus siglas en inglés) es una tecnología prometedora para la captura de CO2.
Objetivo: este estudio tuvo como objetivo evaluar el mineral de manganeso impregnado con Cu (OXMN009P) como un transportador de oxígeno eficaz para este proceso, utilizando específicamente CO y H2 como combustibles.
Metodología: la metodología implicó análisis termogravimétrico (TGA) y pruebas en un reactor de lecho fluidizado discontinuo (bFB) para evaluar el rendimiento del material.
Resultados: los resultados mostraron que OXMN009P exhibió un índice de velocidad de reacción (RI) que oscilaba entre 6.1 y 20.1% /min. También logró altas eficiencias de conversión de combustible, casi el 100% para H2 y aproximadamente el 70% para CO, lo que demuestra una reactividad y capacidad de transporte de oxígeno mejoradas. Además, la vida útil de las partículas se extendió a 2031 horas, lo que reduce significativamente la las reposiciones anuales de inventario de sólidos**.**
Conclusiones: en conclusión, el análisis económico sugiere que el costo del material de OXMN009P no sería un factor limitante para la implementación de la tecnología CLC.

Palabras clave: Transportadores sólidos de oxígeno, Mineral de manganeso, Impregnación de cobre, Indice **de**

How to cite?

Forero, C.M., Arango, E., Velasco, F.J., Peña, S.E. Economic evaluation of Cu-impregnated manganese for CO2 capture in combustion with solid oxygen carriers. Ingeniería y Competitividad, 2025, 27(1)e-20914807

https://doi.org/10.25100/iyc.v27i1.14807

Received: 9/9/24
Reviewed: 10/20/24
Accepted: 02/12/25
Online: 02/14/25

Correspondence
carmen.forero@correounivalle.edu.co

Contribution to the literature

This study was conducted to assess Cu-impregnated manganese ore (OXMN009P) as an oxygen carrier for CO2 capture in Chemical Looping Combustion (CLC), using CO and H2 as fuels. The aim was to advance the utilization of manganese ore as oxygen carriers in CLC and evaluate the economic feasibility of modifying low-cost materials with an active copper phase.

The most relevant results include:
OXMN009P showed high reactivity with a reaction rate index of 6.1 to 20.1% /min.
It demonstrated high fuel conversion efficiencies, nearly 100% for H2 and 70% for CO.
The particle lifetime extended to 2031 hours, which is higher than other reported natural minerals.
Economic analysis revealed that the makeup flow cost per tonne of CO2 avoided was similar for both OXMN009 and OXM-N009P (US$0.28 and US$0.27, respectively).

These results contribute to the following:
They demonstrate that OXMN009P is a promising low-cost, manganese-based oxygen carrier for syngas and solid fuel CLC applications. The improved reactivity and extended particle lifetime achieved through copper impregnation outweigh the increased cost of the material. The economic analysis suggests that material cost would not be a limiting factor for implementing CLC technology with OXMN009P. These findings provide valuable insights into the potential of manganese minerals as oxygen carriers for CLC applications and the economic viability of modifying low-cost materials with an active copper phase.

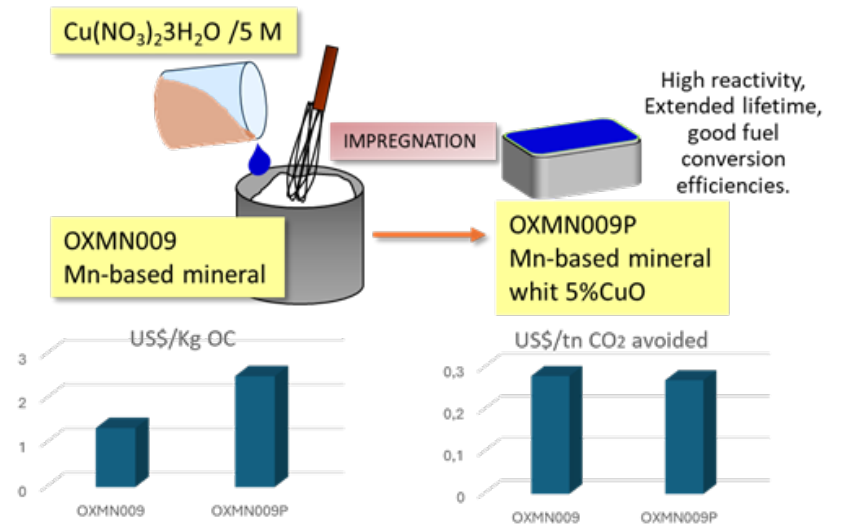

Material cost wouldn't be a limiting factor for implementing CLC technology with OXMN009P

doi: 10.25100/iyc.v27i1.14807

Introduction

Chemical Looping Combustion (CLC) is a promising technology for carbon capture and storage that can be used with carbon-neutral fuels, i.e., biomass or waste streams of agro-industry; which is known as bioenergy with carbon capture storage (BECCS)(1). Generally, CLC consists of two interconnected fluidized bed reactors namely an air reactor (AR) and a fuel reactor (FR), where the oxygen carrier (OC) circulates (see Figure 1).

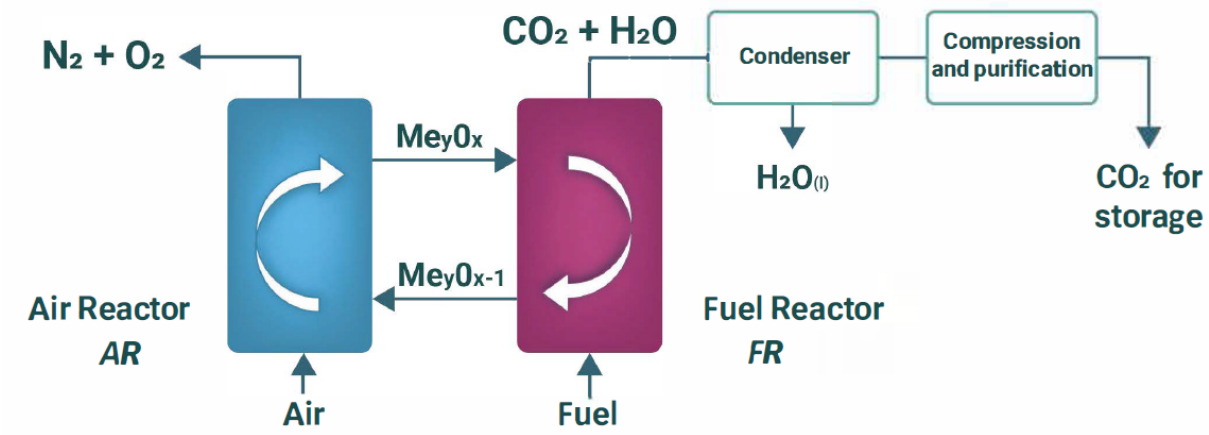

Figure 1. Chemical Looping Combustion - CLC process scheme

In the AR, the OC is oxidized in air presence, avoiding the direct contact between air and fuel, and this reaction can be represented by:

$$Me_xO_{y-1} + O_2 \rightarrow 2Me_xO_y \quad (1)$$

In a CLC system operated with solid fuels, the reactions in the FR follow the following equations:

$$solid\ fuel \rightarrow char + volatiles\ (CH_4, CO\ and\ H_2) \quad (2)$$
$$char + H_2O \rightarrow CO + H_2 + ash \quad (3)$$
$$Me_xO_y + CH_4 + \rightarrow Me_xO_{y-1} + CO + 2H_2 \quad (4)$$
$$Me_xO_y + CO \rightarrow Me_xO_{y-1} + CO_2 \quad (5)$$
$$Me_xO_y + H_2 \rightarrow Me_xO_{y-1} + H_2O \quad (6)$$

This cyclical process eliminates the formation of nitrogen oxides (NOx), resulting in a free flow of nitrogen gas in the FR effluent, which facilitates CO_2 separation by condensing the combustion stream (2).

The OC is crucial for the successful implementation of CLC technology, as its performance relative to other BECCS technologies will significantly impact the overall efficiency and economic viability of the carbon capture process (CCP). Effective OCs must possess a combination of high oxygen-carrying capacity, efficient fuel oxidation, robust reactivity, durability against wear, resistance to carbon formation, excellent fluidization properties, and a minimal environmental footprint.. These characteristics are crucial for the long-term operational stability of CLC systems, where OCs are

doi: 10.25100/iyc.v27i1.14807

typically synthesized by impregnating an active metal oxide onto an inert support. This method enhances mechanical resistance and maintains reactivity (3).

OC resistance to mixing with ash is vital in solid fuel systems because they come into direct contact in the FR. Lack of resistance can lead to agglomeration and reduced reactivity. Preventing ash accumulation requires its removal, which leads to OC losses (4). Therefore, using low-cost materials as OCs is very valuable. In this context, there is a growing interest in identifying low-cost OCs(5-9). Particularly in char gasification CLC with solid fuels, Mn ores have demonstrated higher reactivity compared to ilmenite, as indicated by numerous studies(6, 10-13). However, their performance depends on their origin (Mn concentration and presence of elements such as Fe, Ca, and Si) (14, 15). On the other hand, Ni and Cu-based oxides have practical limitations that restrict their applicability in CLC systems(16-19). These highlight the need for alternative or modified OCs to overcome these challenges and improve CLC efficiency. An example is Mn ores modified with small amounts of Cu, which increase reactivity and prevent agglomeration problems (20-22).

Previous studies have investigated the redox behavior of a low-cost Colombian ore with a high manganese content, in which provides a detailed analysis of the TGA and bFB performance of OXMN009 (23). Therefore, this study aims to advance the utilization of ore manganese as OCs in CLC. To achieve this, OXMN009 was selected as the starting material and modified with copper. The modified OCs (OXMN009P) were then subjected to comprehensive experiments using thermogravimetric analysis (TGA) and a batch fluidized-bed reactor (bFB). The primary focus was to assess the reactivity of these OCs with the components of syngas (CO and H_2), which are the gasification products derived from carbon-based solids.

In order to determine the economic feasibility of modifying the low-cost material with an active copper phase, design criteria were applied. Additionally, a cost comparison between the modified and unprocessed materials was conducted to evaluate the cost of CO_2 avoided. The findings from this study will contribute to a deeper understanding of the potential of manganese minerals as OCs for CLC applications and provide valuable insights into the economic viability of modifying low-cost materials with an active copper phase.

Materials and methods

Building on previous work where Colombian ore OXMN009 showed promise in reacting with syngas components (CO and H_2)(23), this study investigates processing OXMN009 with copper (Cu) using a method established elsewhere(24). Following literature recommendations(20, 22, 25, 26), OXMN009 was infused with 5 wt% CuO via copper nitrate solution. The oxygen carrier was prepared by incipient wetness impregnation. A 5 M solution of copper nitrate trihydrate ($Cu(NO_3)_2 .3H_2O$) was utilized, equivalent to the material's pore volume. The material was calcined at a temperature of 823 K for 30 minutes and then stabilized at 1123 K in an air atmosphere for 1 hour. The resulting material, OXMN009P, was characterized using XRF, XRD (Table 1), SEM (particle morphology, Figure 2), and sieving (size distribution). The details of the techniques used were presented in a previous work(27).

doi: 10.25100/iyc.v27i1.14807

Table 1. Characterization summary of OXMN009 and OXMN009P

Elements (XRF analysis %m/m)						
OC	**SiO_2**	**Fe_2O_3**	**Al_2O_3**	**CaO**	**MnO**	**CuO**
OXMN009	4.78	2.16	0.80	0.19	91.33	0.11
OXMN009P	4.80	1.94	0.64	0.20	87.93	3.92
Main phases (XRD analysis)						
OXMN009	Hausmannite (Mn_3O_4), Bixbyite (Mn_2O_3)					
OXMN009P	Hausmannite (Mn_3O_4), Bixbyite (Mn_2O_3), Teronite (CuO)					

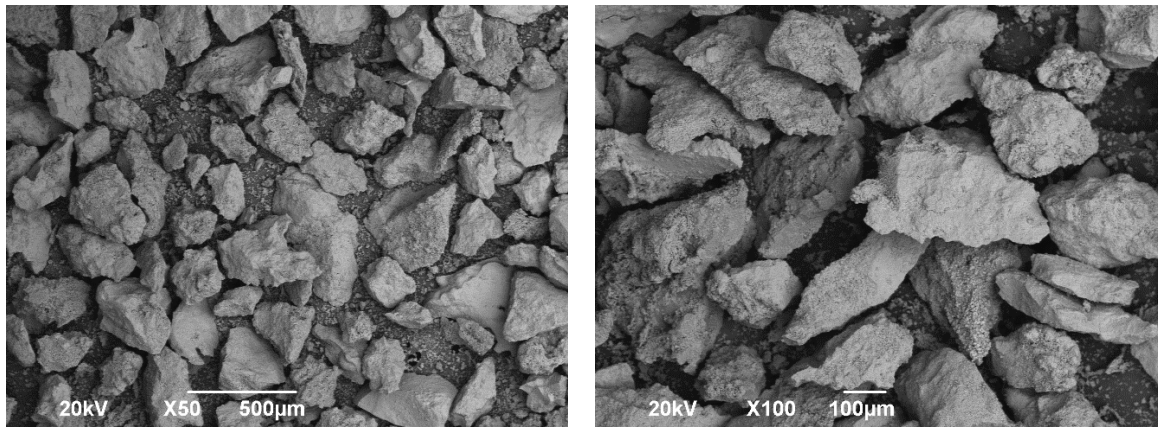

Figure 2. Scanning electron microscopy of OXMN009P at x50 and x100 magnification.

XRD identified hausmannite (Mn_3O_4), bixbyite (Mn_2O_3), and teronite (CuO) in OXMN009P. Literature suggests that Mn_2O_3 is readily reduced to Mn_3O_4, but reoxidation is difficult at temperatures above 800°C. Conversely, Mn_3O_4 can be easily cycled between MnO and Mn_3O_4 through reduction and oxidation(28). No oxygen uncoupling was detected during the post-oxidation purges in the TGA and bFB trials. Consequently, only the Mn_3O_4/MnO and CuO/Cu systems were considered in this study (see Table 2).

Table 2. Redox reactions of the active phase found in OXMN009P

Active phase	**Stage**	**Reactant**	**Reaction**	
CuO	**Reduction**	**CO**	$CuO + CO \rightarrow Cu + CO_2$	(7)
		H_2	$CuO + H_2 \rightarrow Cu + CO_2$	(8)
	Oxidation	**O_2**	$2Cu + O_2 \rightarrow 2CuO$	(9)
Mn_3O_4	**Reduction**	**CO**	$Mn_3O_4 + CO \rightarrow 3MnO + CO_2$	(10)
		H_2	$Mn_3O_4 + H_2 \rightarrow 3MnO + H_2O$	(11)
	Oxidation	**O_2**	$6MnO + O_2 \rightarrow 2Mn_3O_4$	(12)

To evaluate the performance of OXMN009P, a two-phase analysis was conducted. Thermogravimetric analysis (TGA) was performed on small samples of OXMN009P, which were heated in a controlled environment and monitored for weight changes under various conditions (temperature, gas type, concentration). Subsequently, a larger quantity of OXMN009P was tested in

doi: 10.25100/iyc.v27i1.14807

a batch fluidized bed reactor (bFB) to assess its performance under conditions resembling those of actual carbon capture processes.

The experiment and data analysis methods used in this study were adapted from (23). Briefly, the reduction (X_{red}) and oxidation (X_{ox}) conversion curves were generated using the following equations:

$$X_{red} = \frac{m_{ox} - m}{m_{ox} - m_{red}} \quad (13)$$

$$X_{ox} = 1 - \frac{m_{ox} - m}{m_{ox} - m_{red}} \quad (14)$$

Where m_{ox} and m_{red} are the OC masses in the oxidized and reduced state, respectively, and m is the mass at time t.

These equations are the basis for determining some parameters such as:

Oxygen Transport Capacity R_o: How much oxygen the material can absorb and release.

Reaction Rate Indeces RI: How quickly the material reacts with different gases. This parameter is used to compare the performance obtained for the OXMN009P with other OC reported in the literature.

Particle Durability: How well the material resists wear and tear. for which particle lifetime (PL) was estimated.

System Efficiency: The overall performance of the material in a carbon capture process.

Established methods and equations were used to calculate these parameters, based on the data collected during the experiments (23).

Although the particle size of OC is in the range of 300 to 500 µm, due to friction some particles reach a small size (≤ 45 µm), which often have a limited residence time within the CLC system. This leads to their elutriation, allowing for recovery in filters and subsequent quantification to estimate particle lifetime (PL) in hours(29), as calculated by equation:

$$PL = \frac{m_{oc}\Delta t}{m_f * 3600} \quad (15)$$

here m_f is the mass of elutriated particles under 45 µm in a time Δt (expressed in seconds), and m_{oc} is the total mass of OC fed into the system (solid inventory).

The main parameters for the design of a CLC system are: (i) circulation velocity of OC between the reactors, (ii) amount of OC in the bed of the reactors, and (iii) gas leakage between the reactors should be minimum(30).

doi: 10.25100/iyc.v27i1.14807

The first two parameters are known as recirculation velocity (m^*_{oc}) and solid inventory (m_{oc}), and these are characteristics of the OC used (reactivity, type of metal oxide, oxygen transport capacity, etc.) and can be determined employing the following methodology proposed in the literature(31), from which equations (16) through (22) were obtained.

The solid inventory required for transferring oxygen in the FR and AR depends on OC reactivity in the redox reactions. For preliminary estimations, the mass transfer effects in the bFB are neglected. For a complete gas conversion, the amount of OC in each reactor for 1 MW of fuel can be estimated for the following equations:

$$m_{OC,j} = m_c^* \left(\frac{\tau_i}{\Phi_j}\right) \quad (16)$$

Where characteristic cir$_{\Phi_j}$lation rate, m_c^*, is a specific parameter defined by the OC-fuel pair, and the characteristic reactivity (j=FR or AR as appropriate) is defined by:

$$\Phi_j = \left[\tau_{ir}\left(\frac{\overline{dX}}{dt}\right)\right]_j \quad (17)$$

The total conversion time τ_{ij} in redox reactions to the reactive gas average concentration in FR and AR is determined by equation (24). Assuming a perfect mixture of solids, plug flow in the reactors, and no resistance to gas exchange between the bubble and emulsion phases in the fluidized bed, the average concentration of reactive gas in each reactor can be obtained as a function of the conversion of gas, X_g, by equation (18).

$$\overline{C_g}^n = \frac{\Delta X_g C_0^n}{\int_{X_{g,in}}^{X_{g,out}} \left[\frac{1+\varepsilon_g X_g}{(1-X_g)}\right] dX_g} \quad (18)$$

Where ε_g is the volumetric expansión of the gas after reaction, assuming an ideal gas model and a constant temperature in the reactor can be determined as:

$$\varepsilon_g = \frac{V_{g,X_g=1} - V_{g,X_g=0}}{V_{g,X_g=0}} \quad (19)$$

The value of ε_g is equal to zero for the combustion of H_2 and CO, but in the oxidation reaction with air, it equals -0.21. Assuming a perfect mix of solid particles in the bFB, Φ_j can be expressed in each reactor as a function of the average conversion of the solid in the inlet, $\overline{X}_{i,E\,j}$ (i=o: oxidation or r: reduction as appropriate) and the conversion change ΔX for the following equations:

For plate-like geometry:

$$\Phi_j = 1 - \exp\left(-\frac{1-X_{o,in\,j}}{\Delta X}\Phi_j\right) \quad (20)$$

For spheral grain particles:

doi: 10.25100/iyc.v27i1.14807

$$\Phi_j = 3\left[1-\overline{X}_{0,in,j}^{\frac{2}{3}}\exp\left(-\frac{1-\overline{X}_{o,in\,j}^{\frac{1}{3}}}{\Delta X}\Phi_j\right)\right]-\frac{6\Delta X}{\Phi_j}\left[1-\overline{X}_{o,in,j}^{\frac{1}{3}}\exp\left(-\frac{1-\overline{X}_{o,in,j}^{\frac{1}{3}}}{\Delta X}\Phi_j\right)\right] - \frac{6\Delta X^2}{\Phi_j^2}\left[1-\exp\left(-\frac{1-\overline{X}_{o,in,j}^{\frac{1}{3}}}{\Delta X}\Phi_j\right)\right] \quad (21)$$

For the determination of the solid inventory, the Φ_j is a helpful parameter because it is the only function of $\overline{X}_{i,E\,j}$, and ΔX, in addition to being valid for any reactivity and R_O of the OC. It is important to note that the term Φ_j takes values between 0 and 3 for spherical particles and between 0 and 1 for plate-like particles. Finally, the solids inventory, m_{TSO}, in a CLC system for a 1 MW of fuel, will be given by:

$$m_{OC} = m_{OC,FR} + m_{OC,AR} \quad (22)$$

Results

Oxygen Carrier behavior in thermogravimetric analysis

The TGA data, showing mass variation over time, allowed for calculating OC conversions under various operating conditions using equations (13) and (14). As expected in an exothermic system, reactivity increased proportionally with temperature (see Figure 3). Also, the reactivity is expected to increase with the temperature for endothermic reactions, unless thermodynamic equilibrium limits the reaction which is not the case. Additionally, higher reactant concentrations positively influenced the reaction rate in the redox reactions. (see Figure 4).

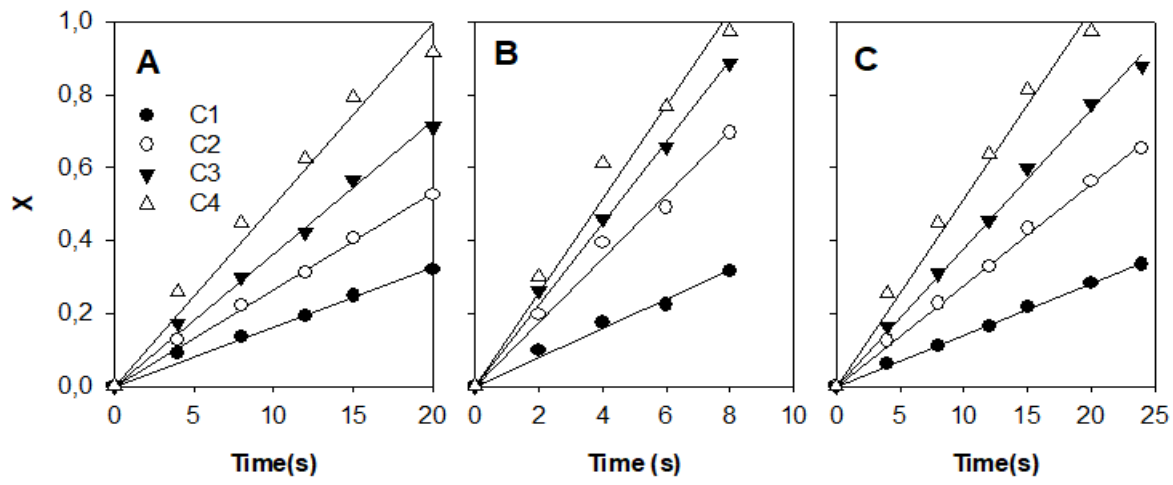

Figure 3. Effect of temperature on the OXMN009P conversion X with respect to time, using reactants: A) 25 %v/v CO and N_2 balance; B) 25 %v/v H_2 and N_2 balance; C) oxidation: 100 %v/v air.

doi: 10.25100/iyc.v27i1.14807

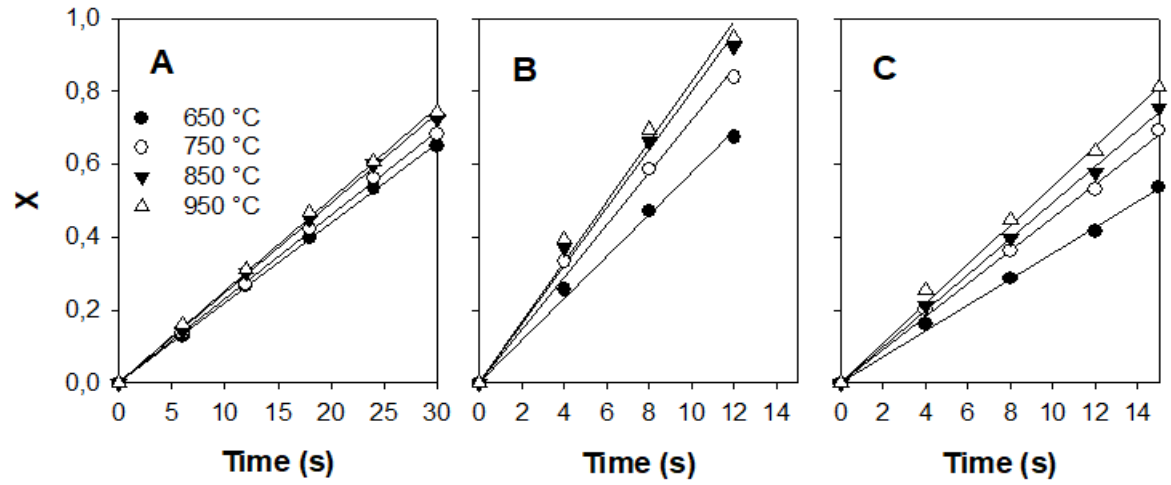

Figure 4. Effect of reactant concentration on the OXMN009P conversion X as a function of time, using reactants: A) C1 = 15, C2 = 25, C3 = 35, and C4 = 50 %v/v of CO and N_2 balance; B) C1 = 15, C2 = 25, C3 = 35, and C4 = 50 %v/v of H_2, and N_2 balance; C) C1 = 5, C2 = 10, C3 = 15, and C4 = 21 %v/v of O_2 and N_2 balance. T = 950 °C.

The RI_{TGA} obtained for OXMN009P and the values reported by other authors for low-cost materials based on Mn are summarized in Table 3, it can be observed that the values obtained with CO and H_2 are within the range indicated by other authors for low-cost Mn-based materials and shows that Cu impregnation improves the reactivity of the material.

Table 3. RI_{TGA} (%/min) in tests at 950 °C of OXMN009 and low-cost materials based on Mn reported by other authors. [a] Calcined material. [b] material used.

RI_{TGA} (%/min)			
Material	**CO**	**H_2**	**O_2**
OXMN009(23)	5.8 [a]	15.1 [a]	12.5
OXMN009P	6.1 [a]	20.1 [a]	13.8
OXMN010A(27)	17.9	38.8	-
Mn Ores (15)	5.1-9.0[a](1.4-5.3)[b]	14.2-26.4 (9.0-14.8)	8.4-11.3 (8.1-9.9)

To verify the OXMN009P reaction stability as a function of the number of cycles, an experimental RI_{TGA} of 20 consecutive cycles was performed in TGA. Reaction stability was satisfactory since the and R_O do not change through cycles. This behavior is similar to results obtained for OXMN009 and OXMN010A in previous studies(27). It is worth highlighting that the R_O ,exp values for Mn-ore showed a slight increase after Cu impregnation, before impregnation, ,exp was 7.0% m/m, and after impregnation, it increased to 7.5 % m/m(32).

doi: 10.25100/iyc.v27i1.14807

Reaction kinetics

Reaction kinetic parameters were determined by fitting the conversion-time data to a shrinking core model (SCM), a widely used model for describing OC redox kinetics under gaseous environments.(27, 33, 34). This model posits that, as the reaction progresses, the core of the metal oxide phase shrinks towards the particle's center, forming a porous product layer through which gaseous reactants and products diffuse. The adjustment of the SCM was carried out assuming that the particles have a plate-like geometry based on the visual information given for the SEM microscopies (see Figure 2) using the following equations:

$$\frac{t}{\tau_j} = X_j \qquad (23)$$

where τ_j is the total conversion time of reaction j, which can be determined as:

$$\tau_j = \frac{\rho_m L}{\bar{b} k C_g^n} \qquad (24)$$

Equation (24) determining the specific rate constant (k), the activation energy (E_a) and pre-exponential factor (k_0) can be calculated as functions of temperature, assuming Arrhenius kinetics are followed. This model applies to many reactions (35).

$$k = k_0 e^{\left(\frac{-E_a}{RT}\right)} \qquad (25)$$

By logarithmically linearizing equation (24), the reaction order for each reaction j can be determined through a least-squares fit of ln(k) against ln(C). Similarly, equation (25) allows for the calculation of activation energies by fitting ln(τ_j) against 1/T (Figure 5.A and Figure 5. B)

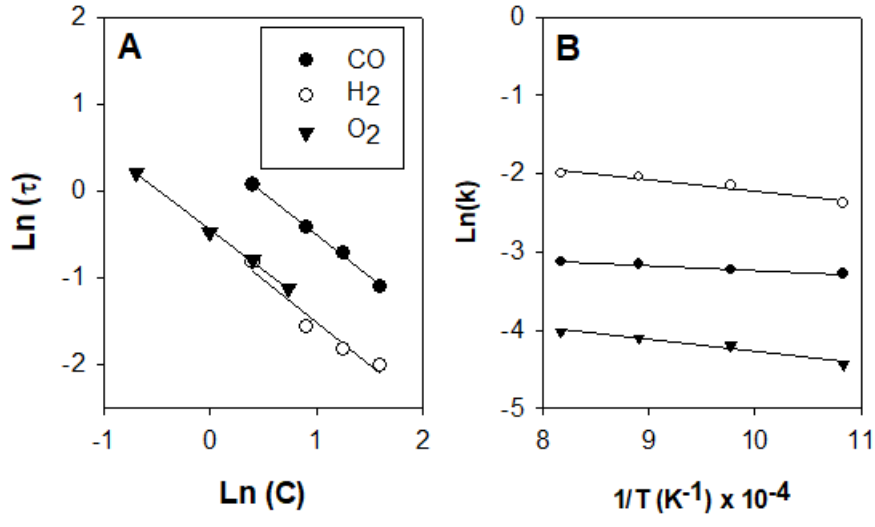

Figure 5. A. Linear fits to determine the reaction orders (n). B. Linear fits to determine activation energies (E_a) and pre-exponential factors (k_0)

doi: 10.25100/iyc.v27i1.14807

The kinetic parameters obtained for n OXMN009P, using CO, H_2, and O_2 as reactive gases, are summarized in Table 3. The values for E_a are within the interval reported in the literature for Mn-based OCs (0.65 to 1.2)(27, 36-38). The values obtained for OXMN009P are between 5.0 and 12.8 kJ/mol, an interval lower than the reported for synthetic and low-cost OCs of Fe, Cu, Ni, and Mn (10.2 to 80.7 kJ/mol)(27, 36, 39, 40).

Table 3. Kinetic parameters of OXMN009P

Reactant	Concentration (% v/v)	n	E_a (kJ/mol)	Temperature (°C)	k_0 ((m/s)(mol/m³)$^{1-n}$)
CO	15 – 50	1.0	5.0	650 - 950	0.07
H_2	15 – 50	1.0	12.1	650 - 950	0.46
O_2	5 – 21	0.9	12.8	650 - 950	0.06

Oxygen carrier behavior in batch fluidized bed reactor (bFB)

OXMN009P evaluation in bFB was carried out, and the distribution of gases in the outlet is shown in Figure 6. This data allowed calculation of the rate index, fuel conversions, and OC conversions with equations 9 to14 of previous work (23) , and the results are summarized in Ta RI_{TGA} The fuel conversions rea RI_{bFB} with H_2 are higher than with CO, which is consistent with the values found, and the are within the interval reported in the literature for other Mn-based OCs(14,

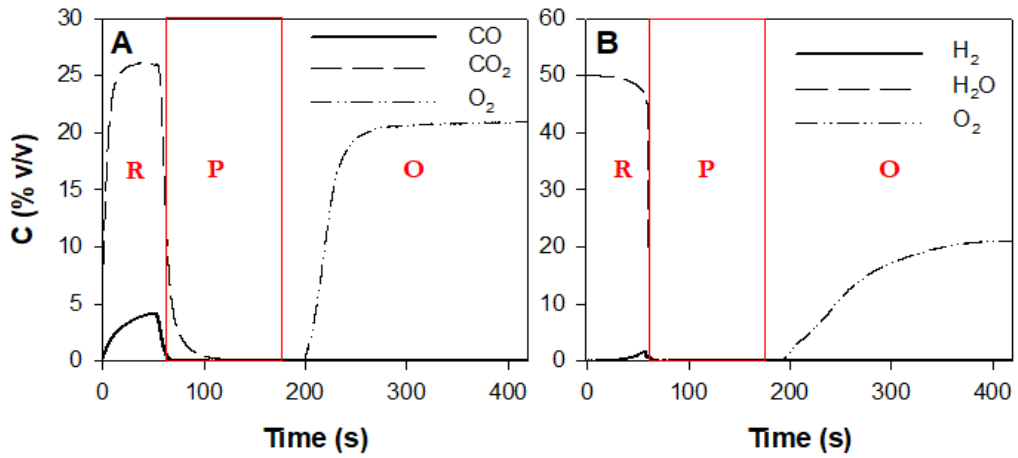

Figure 6. Gas product composition during reduction (R), purge (P), and oxidation (O) in the bFB reactor for OXMN009 at 950 °C. A. Reduction: 25 %v/v CO, 10 % CO_2 with N_2 balance; purge 100 %v/v N_2; oxidation 100 %v/v air. B. Reduction: 50 %v/v H_2 with N_2 balance; purge 100 %v/v N_2; oxidation 100 %v/v air.

doi: 10.25100/iyc.v27i1.14807

Table 4. Summary of the bFB test results.

Materials	Reactive	RI	X_{Fuel} (%)
OXMN009	CO	0.9	69.7
	H_2	1.6	99.1
OXMN009P	CO	1.5	90.3
	H_2	1.7	99.3
OXMN010A(41)	CO	1.4	99
	H_2	1.3	92
Mn Ores(15)	CO	0.4 – 1.0	
	H_2	1.5 – 2.0	99
Mn Ores(14)	CH_4		5 - 80
	Syngas		50 – 90

By measuring the mass of material elutriated from the bFB reactor and captured by the effluent filter, an approximate particle lifetime (PL) was estimated using equation (15). This resulted in a value of 2031 hours for OXMN009P, which exceeds those reported in the literature for other natural minerals (150-1600 hours) (8, 15, 42, 43) and is higher than OXMN009, which was 1531h. In our experiments, the fluidization number was set to 3 , which corresponds to a superficial gas velocity in the range of 0.09 m/s – 0.12 m/s. Typical superficial gas velocities in a CLC unit are over 4 m/s. This considerable difference in velocities should be noted, as it implies that the lifetime of materials observed in our batch experiments will not correspond to the actual lifetime in a CLC plant. Anyway, the attrition rate observed in the batch fluidized bed serves as a comparative parameter to evaluate the performance of different oxygen carrier materials. Once steady-state operating conditions were established, the reactor's differential pressure remained relatively constant, suggesting the absence of agglomeration issues among the OXMN009P particles.

Design criteria

From the kinetic data obtained in previous sections, the solids inventory, m_{OC}, was determined for the OXMN009P. The recirculation velocity, m^*_{OC}, and the m_{OC} have an inverse dependence; however, m^*_{OC} must not be higher than $16\ kg\ s^{-1}\ MW$ to avoid an increase in operating costs(31).

The literature report that the minimum m_{OC} in a CLC system is obtained for an intermediate situation between OC complete reduction in FR and OC oxidation in AR (31, 33, 36), for which the input conversion in the AR was determined as $\overline{X}_{AR,in} = 0.5 + \Delta X/2$ (44). With the ΔX and $\overline{X}_o$ obtained, the characteristic reactivities, Φ_j, were estimated using equation (20) for like-plate geometry.

Reactive gas average concentration in each reactor, $\overline{C}_g$, were obtained using equation (18), assuming a 100 % fuel (CO or H_2) in the inlet of FR, the efficiency of combustion of 99.9 %, and an air excess of 20 % in AR. With the $\overline{C}_g$ values, the τ_i at 950 °C was determined, and finally, the minimum solids inventory for each reactor was estimated. The results are presented in Table 5.

doi: 10.25100/iyc.v27i1.14807

Table 5. Minimum solids inventory, m_{OC} (kg/MW), required in a CLC system to achieve 99.9% CO and H_2 combustion efficiency at 950 °C. Oxidation: air 100%.

Material	Fuel	ΔX	$\overline{X}_{o,in,RO}$	$\overline{C}_{g,RR}$	$\overline{C}_{g,RO}$	τ_r (s)	τ_o(s)	$m_{OC,RR}$	$m_{OC,RO}$	m_{OC}
OXMN009	**CO**	0.05	0.47	12.6%	11.1%	85	41	69	33	102
	H_2	0.06	0.47	12.2%	11.1%	40	41	38	39	77
OXMN009P	**CO**	0.05	0.48	15.2%	11.1%	48	26	48	26	74
	H_2	0.06	0.47	14.7%	11.1%	20	34	18	30	48

The minimum m_{OC} obtained for OXMN009 are in the interval reported in the literature for Mn-based minerals, 97 to 275 kg/MW for combustion with CO and 69 to 85 kg/MW with H_2 as fuel (15); nevertheless, OXMN009P has better values, similar to reported for synthetic OC based on Cu and Fe (50 – 87 kg/MW and 37 – 72 kg/MW for CO and H_2 respectively)(31). Results indicated a decrease of m_{OC} in the Cu-processed material, which leads to lower costs in the implementation and operation of the CLC system. It is important to note that the minimum solids inventory values presented here are theoretical and assume ideal conditions without mass transfer limitations. In practical applications, the actual solids inventory required may be significantly higher, potentially 2-10 times greater, as reported in the literature(45).

In addition to the properties studied in the previous sections, another essential characteristic of an OC is the economic cost, especially for synthetic materials. The cost of an OC is the sum of several factors, including the cost of the metal oxides, the inert support, the transportation costs of raw materials, and the cost of manufacturing. However, when preparation methods are used on an industrial scale, the manufacturing costs of the OC are negligible, and the final cost is given mainly by the price of the raw materials(46), which the cost of the OC, c_{oc}, can be expressed as follows:

$$c_{OC} = x_{Cu}c_{Cu} + (1 - x_{Cu})c_{Mn} + c_m \quad (26)$$

Where x_{Cu} is the mass fraction of Cu impregned, c_{Cu} is the cost of solution of copper nitrate trihydrate necessary to produce OXMN009P, c_{Mn} is the cost of Mn ore(47) and c_m is the manufacture cost of the oxygen carrier (31), in US$/kg. From the average costs for 2023, the c_{oc} was determined using the equation 26 and obtained values of 2.5 US$/kg for OXMN009P and 1.33 US$/kg for OXMN009. The c_{oc} increased almost 2 times due to Cu content; however, other operational factors are necessary for a proper economic comparison. Among the materials used as OC, the Mn-based minerals are the cheapest, compared with values reported in the literature(48-49), whereby the OXMN009 and OXMN009P are excellent candidates for CLC technology.

The major advantage of the CLC process over other BECCS technologies is that it eliminates the need for additional separation of CO_2 from the flue gas. Consequently, the cost per tonne of CO_2 avoided depends primarily on the losses occurring during the redox cycles (31). The cost of the makeup flow of oxygen carrier OC per tonne of CO_2 avoided (χ_{oc}) can then be estimated by:

$$\chi_{OC} = 10^3 \mu^*_{0,OC} c_{OC} \quad (27)$$

doi: 10.25100/iyc.v27i1.14807

where $\mu^*_{0,oc}$ is the flow of new OC added (kg/s) per kg/s of CO_2 avoided, this parameter is a function of the m_{oc}, the particle lifetime (PL), and the fuel combustion enthalpy (ΔH^0_c) and can be calculated with the following equations:

$$\mu^*_{0,oc} = \frac{\mu_{oc}}{PL} \quad (28)$$

$$\mu_{oc} = \frac{\Delta H^0_c}{s_e M_{CO_2}} m_{oc} \quad (29)$$

The solids inventory required per kg/s of CO_2 avoided, μ_{co}, depends on the mols number of CO_2 produced per mol. Assuming a syngas with 50 %v/v CO and 50 %v/v H_2, the specific emission, s_e defined as the moles of CO_2 produced per mol of fuel gas is equals 0.5, and ΔH^0_c equals -0.2829 MJ/mol, the results presented in Table 6 are obtained.

Table 6. Results of economic analysis of the study materials.

Material	μ_{oc} (kg/(kg/s of CO_2 avoided))	μ^*_{oc} (kg/s /(kg/s of CO_2 avoided))	χ_{oc} (US$/ton of CO_2 avoided)
OXMN009	1151	2.1 E-04	0.28
OXMN009P	784	1.1 E-04	0.27

The χ_{oc} obtained for OXMN009P is similar to OXMN009. This suggests that the impregnation process did not significantly impact the economic benefits when considering CO_2 avoided as the evaluation criterion. Based on literature, other operational aspects and equipment costs associated with implementing a 5 MWth CLC plant using OXMN009P might improve the makeup flow cost per tonne of CO_2 avoided (49). However, achieving this goal requires detailed engineering analysis, specific project data, and access to industry-standard cost estimation references and databases.

Conclusions

This work successfully synthesized and evaluated OXMN009P, a low-cost, Colombian-derived manganese-based oxygen carrier with promising results for syngas and solid fuel CLC aplications. TGA and bFB tests with CO and H_2 as fuels indicate its potential due to high reactivity, extended lifetime, and good fuel conversion efficiencies.

An economic analysis based on material costs revealed that the makeup flow of oxygen carrier OC per tonne of CO_2 avoided was similar for both OXMN009 and OXMN009P (US$0.28 and US$0.27, respectively). Although the synthesized OXMN009P is twice as expensive as manganese ore, the improved reactivity and particle lifetime achieved through copper impregnation outweigh this cost difference. Therefore, the economic analysis suggests that material cost wouldn't be a limiting factor for implementing CLC technology with OXMN009P.

doi: 10.25100/iyc.v27i1.14807

Appendix. Nomenclature

AR: Air reactor
BCCS: Bioenergy CO_2 capture and storage
bFB: Batch fluidized bed reactor
CCP: Carbon capture process
CLC: Chemical looping combustion
c_{Cu}: Cost of solution of copper nitrate trihydrate
$\overline{C_g}$: average concentration of reactive gas in each reactor
c_{Mn}: Cost of Mn ore
c_m: Manufacture cost of the oxygen carrier
c_{OC}: Cost of the OC
E_a: Activation energy
FR: Fuel reactor
k: Specific rate constant
k_0: Pre-exponential factor
L: Length of flat particle
m: Mass of the OC at time t
m_c^*: characteristic circulation rate
m_f: Mass of elutriated particles under 45 µm in a time Δt
m_{OC}: Total mass of the OC fed into the system
$m_{OC,j}$: Solid inventory required for transferring oxygen in the FR and AR
m_{ox}: Mass of the OC oxidized state
m_{red}: Mass of the OC reduced state
n: Reaction order
OC: Solid oxygen carrier
PL: Particle lifetime
p_{TGA}: Partial pressure of the fuel in the TGA
R: Universal gas constant
RI: Reaction rate index
RI_{TGA}: Reaction rate index in TGA test
RI_{bFB}: Reaction rate index in bFB test
R_O: Oxygen transport capacity
SCM: Shrinking core model
SEM: Scanning electron microscopy
T: Temperature
t: Time
TGA: Thermogravimetric analysis
XRD: X-ray diffraction
XRF: X-ray fluorescence
x_{Cu}: Mass fraction of Cu impregned
X_g: Conversion of gas
$\overline{X}_{i,E\,j}$: Average conversion of the solid in the inlet (i=o: oxidation or r: reduction)

doi: 10.25100/iyc.v27i1.14807

X_{ox}: OC conversion in oxidation
X_{red}: OC conversion in reduction

Greek letters

ε_g: Volumetric expansión of the gas after reaction
ΔX: OC conversion change
Φ_j: characteristic reactivity in j= FR or AR
ρ_m: Molar density of the OC active phase
τ_j: Total conversion time (j=o: oxidation or r: reduction)

Acknowledgments

The authors gratefully acknowledge the financial support provided by the Colombia Scientific Program within the framework of the call Ecosistema Científico (Contract No. FP44842- 218-2018). Also, the financial support of COLCIENCIAS through the Contingent Recovery Contract FP44842-14-2017 and the Laboratorio Combustión Combustibles of the Universidad del Valle.

CRediT authorship contribution statement

Conceptualization - Ideas: Carmen Rosa Forero Amórtegui. Data Curation: Sandra Emperatriz Peña, Eduardo Arango Durango. Formal analysis: Carmen Rosa Forero Amórtegui, Sandra Emperatriz Peña, Eduardo Arango Durango. Acquisition of funding: Carmen Rosa Forero Amórtegui, Francisco Javier Velasco Sarria. Investigation: Carmen Rosa Forero Amórtegui, Sandra Emperatriz Peña, Eduardo Arango Durango. Methodology: Carmen Rosa Forero Amórtegui, Sandra, Emperatriz Peña, Eduardo Arango Durango, Francisco Javier Velasco Sarria. Project Management: Carmen Rosa Forero Amórtegui. Resources: Carmen Rosa Forero Amórtegui, Francisco Javier Velasco Sarria Supervision: Carmen Rosa Forero Amórtegui, Francisco Javier Velasco Sarria. Validation: Sandra Emperatriz Peña, Eduardo Arango Durango. Visualization - Preparation: Carmen Rosa Forero Amórtegui. Writing - original draft - Preparation: Carmen Rosa Forero Amórtegui. Writing - revision and editing - Preparation: Carmen Rosa Forero Amórtegui.

Financing: does not declare
Conflict of interest: does not declare
Etics aspects: does not declare

References

1. Mendiara T, Gayán P, García-Labiano F, de Diego LF, Pérez-Astray A, Izquierdo MT, et al. Chemical Looping Combustion of Biomass: An Approach to BECCS. Energy Procedia. 2017;114:6021-9. https://doi.org/10.1016/j.egypro.2017.03.1737

2. Lyngfelt A, Hedayati A, Augustsson E. Fate of NO and Ammonia in Chemical Looping Combustion—Investigation in a 300 W Chemical Looping Combustion Reactor System. Energy & Fuels. 2022;36(17):9628-47. https://doi.org/10.1021/acs.energyfuels.2c00750

3. Gayán P, Forero CR, Abad A, de Diego LF, García-Labiano F, Adánez J. Effect of Support on the Behavior of Cu-Based Oxygen Carriers during Long-Term CLC Operation at Temperatures above 1073 K. Energy & Fuels. 2011;25(3):1316-26. https://doi.org/10.1021/ef101583w

4. Mendiara T, Gayán P, Abad A, García-Labiano F, de Diego LF, Adánez J. Characterization for disposal of Fe-based oxygen carriers from a CLC unit burning coal. Fuel Processing Technology. 2015;138:750-7. https://doi.org/10.1016/j.fuproc.2015.07.019

5. Linderholm C, Schmitz M, Knutsson P, Lyngfelt A. Chemical-looping combustion in a 100-kW unit using a mixture of ilmenite and manganese ore as oxygen carrier. Fuel. 2016;166:533-42. https://doi.org/10.1016/j.fuel.2015.11.015

6. Mei D, Soleimanisalim AH, Linderholm C, Lyngfelt A, Mattisson T. Reactivity and lifetime assessment of an oxygen releasable manganese ore with biomass fuels in a 10 kWth pilot rig for chemical looping combustion. Fuel Processing Technology. 2021;215:106743. https://doi.org/10.1016/j.fuproc.2021.106743

7. Ströhle J, Orth M, Epple B. Chemical looping combustion of hard coal in a 1 MWth pilot plant using ilmenite as oxygen carrier. Applied Energy. 2015;157:288-94. https://doi.org/10.1016/j.apenergy.2015.06.035

8. Schmitz M, Linderholm C, Hallberg P, Sundqvist S, Lyngfelt A. Chemical-Looping Combustion of Solid Fuels Using Manganese Ores as Oxygen Carriers. Energy & Fuels. 2016;30(2):1204-16. https://doi.org/10.1021/acs.energyfuels.5b02440

9. Pérez-Astray A, Mendiara T, de Diego LF, Abad A, García-Labiano F, Izquierdo MT, et al. Improving the oxygen demand in biomass CLC using manganese ores. Fuel. 2020;274:117803. https://doi.org/10.1016/j.fuel.2020.117803

10. Linderholm C, Lyngfelt A, Cuadrat A, Jerndal E. Chemical-looping combustion of solid fuels - Operation in a 10 kW unit with two fuels, above-bed and in-bed fuel feed and two oxygen carriers, manganese ore and ilmenite. Fuel. 2012;102(0):808. https://doi.org/10.1016/j.fuel.2012.05.010

11. Frohn P, Arjmand M, Azimi G, Leion H, Mattisson T, Lyngfelt A. On the high-gasification rate of Brazilian manganese ore in chemical-looping combustion (CLC) for solid fuels. AIChE Journal. 2013;59(11):4346-54. https://doi.org/10.1002/aic.14168

12. Keller M, Leion H, Mattisson T. Mechanisms of Solid Fuel Conversion by Chemical-Looping Combustion (CLC) using Manganese Ore: Catalytic Gasification by Potassium Compounds. Energy Technology. 2013;1(4):273-82. https://doi.org/10.1002/ente.201200052

doi: 10.25100/iyc.v27i1.14807

13. Arjmand M, Leion H, Mattisson T, Lyngfelt A. Investigation of different manganese ores as oxygen carriers in chemical-looping combustion (CLC) for solid fuels. Applied Energy. 2014;113:1883-94. https://doi.org/10.1016/j.apenergy.2013.06.015

14. Sundqvist S, Arjmand M, Mattisson T, Rydén M, Lyngfelt A. Screening of different manganese ores for chemical-looping combustion (CLC) and chemical-looping with oxygen uncoupling (CLOU). International Journal of Greenhouse Gas Control. 2015;43:179-88. https://doi.org/10.1016/j.ijggc.2015.10.027

15. Mei D, Mendiara T, Abad A, de Diego LF, García-Labiano F, Gayán P, et al. Evaluation of Manganese Minerals for Chemical Looping Combustion. Energy & Fuels. 2015;29(10):6605-15. https://doi.org/10.1021/acs.energyfuels.5b01293

16. Siriwardane R, Tian H, Richards G, Simonyi T, Poston J. Chemical-looping combustion of coal with metal oxide oxygen carriers. Energy & Fuels. 2009;23(8):3885-92. https://doi.org/10.1021/ef9001605

17. Mattisson T, Järdnäs A, Lyngfelt A. Reactivity of some metal oxides supported on alumina with alternating methane and oxygen - Application for chemical-looping combustion. Energy and Fuels. 2003;17(3):643-51. https://doi.org/10.1021/ef020151i

18. Cho P, Mattisson T, Lyngfelt A. Carbon formation on nickel and iron oxide-containing oxygen carriers for chemical-looping combustion. Industrial and Engineering Chemistry Research. 2005;44(4):668-76. https://doi.org/10.1021/ie049420d

19. de Diego LF, García-Labiano F, Adánez J, Gayán P, Abad A, Corbella BM, et al. Development of Cu-based oxygen carriers for chemical-looping combustion. Fuel. 2004;83(13):1749-57. https://doi.org/10.1016/j.fuel.2004.03.003

20. Mungse P, Saravanan G, Uchiyama T, Nishibori M, Teraoka Y, Rayalu S, et al. Copper-manganese mixed oxides: CO2-selectivity, stable, and cyclic performance for chemical looping combustion of methane. Physical Chemistry Chemical Physics. 2014;16(36):19634-42. https://doi.org/10.1039/C4CP01747A

21. Xu L, Edland R, Li Z, Leion H, Zhao D, Cai N. Cu-Modified Manganese Ore as an Oxygen Carrier for Chemical Looping Combustion. Energy & Fuels. 2014;28(11):7085-92. https://doi.org/10.1021/ef5017686

22. Mohammad Pour N, Leion H, Rydén M, Mattisson T. Combined Cu/Mn Oxides as an Oxygen Carrier in Chemical Looping with Oxygen Uncoupling (CLOU). Energy & Fuels. 2013;27(10):6031-9. https://doi.org/10.1021/ef401328u

23. Durango EA, Forero CR, Velasco-Sarria FJ. Use of a Low-Cost Colombian Manganese Mineral as a Solid Oxygen Carrier in Chemical Looping Combustion Technology. Energy & Fuels. 2021;35(15):12252-9. https://doi.org/10.1021/acs.energyfuels.1c00587

doi: 10.25100/iyc.v27i1.14807

24. Forero CR, Gayán P, de Diego LF, Abad A, García-Labiano F, Adánez J. Syngas combustion in a 500 Wth chemical-looping combustion system using an impregnated Cu-based oxygen carrier. Fuel Processing Technology. 2009;90(12):1471-9. https://doi.org/10.1016/j.fuproc.2009.07.001

25. Xu L, Sun H, Li Z, Cai N. Experimental study of copper modified manganese ores as oxygen carriers in a dual fluidized bed reactor. Applied Energy. 2016;162:940-7. https://doi.org/10.1016/j.apenergy.2015.10.167

26. Orrego AJ. Tesis de maestría: Preparación y caracterización de transportadores sólidos de oxígeno basados en Fe y Mn modificados con CuO para combustión con captura de CO2. Cali: Universidad del Valle; 2017. https://bibliotecadigital.univalle.edu.co/server/api/core/bitstreams/986adb2e-42f8-4c52-a552-73a55244fa21/content

27. Velasco-Sarria FJ, Forero CR, Arango E, Adánez J. Reduction and Oxidation Kinetics of Fe-Mn-Based Minerals from Southwestern Colombia for Chemical Looping Combustion. Energy & Fuels. 2018;32(2):1923-33. https://doi.org/10.1021/acs.energyfuels.7b02188

28. Stobbe ER, de Boer BA, Geus JW. The reduction and oxidation behaviour of manganese oxides. Catalysis Today. 1999;47(1-4):161-7. https://doi.org/10.1016/S0920-5861(98)00296-X

29. Cabello A, Gayán P, García-Labiano F, de Diego LF, Abad A, Adánez J. On the attrition evaluation of oxygen carriers in Chemical Looping Combustion. Fuel Processing Technology. 2016;148:188-97. https://doi.org/10.1016/j.fuproc.2016.03.004

30. Lyngfelt A, Leckner B, Mattisson T. A fluidized-bed combustion process with inherent CO2 separation; application of chemical-looping combustion. Chemical Engineering Science. 2001;56(10):3101-13. https://doi.org/10.1016/S0009-2509(01)00007-0

31. Abad A, Adánez J, García-Labiano F, de Diego LF, Gayán P, Celaya J. Mapping of the range of operational conditions for Cu-, Fe-, and Ni-based oxygen carriers in chemical-looping combustion. Chemical Engineering Science. 2007;62(1-2):533-49. https://doi.org/10.1016/j.ces.2006.09.019

32. Arango E, Vasquez FG. Determinación de los parámetros cinéticos para la combustión usando minerales del suroccidente colombiano como transportadores sólidos de oxígeno. Cali-Colombia: Universidad del Valle; 2016. https://bibliotecadigital.univalle.edu.co/server/api/core/bitstreams/7db2177b-3ec5-430b-86e4-8b683b521baf/content

33. García-Labiano F, de Diego LF, Adánez J, Abad A, Gayán P. Reduction and oxidation kinetics of a copper-based oxygen carrier prepared by impregnation for chemical-looping combustion. Industrial and Engineering Chemistry Research. 2004;43(26):8168-77. https://doi.org/10.1021/ie0493311

34. Son SR, Kim SD. Chemical-looping combustion with NiO and Fe2O3 in a thermobalance and circulating fluidized bed reactor with double loops. Industrial & Engineering Chemistry Research. 2006;45(8):2689-96. https://doi.org/10.1021/ie050919x

35. Fogler HS. Elements of Chemical Reaction Engineering: Prentice Hall PTR; 2006. https://books.

doi: 10.25100/iyc.v27i1.14807

google.com.co/books?id=xuHFGWkuxJsC

36. Zafar Q, Abad A, Mattisson T, Gevert B, Strand M. Reduction and oxidation kinetics of Mn3O4/Mg-ZrO2 oxygen carrier particles for chemical-looping combustion. Chemical Engineering Science. 2007;62(23):6556-67. https://doi.org/10.1016/j.ces.2007.07.011

37. Perreault P, Patience GS. Chemical looping syngas from CO2 and H2O over manganese oxide minerals. The Canadian Journal of Chemical Engineering. 2016;94(4):703-12. https://doi.org/10.1002/cjce.22432

38. Ksepko E, Babiński P, Nalbandian L. The redox reaction kinetics of Sinai ore for chemical looping combustion applications. Applied Energy. 2017;190:1258-74. https://doi.org/10.1016/j.apenergy.2017.01.026

39. Abad A, García-Labiano F, de Diego LF, Gayán P, Adánez J. Reduction kinetics of Cu-, Ni-, and Fe-based oxygen carriers using syngas (CO + H2) for chemical-looping combustion. Energy and Fuels. 2007;21(4):1843-53. https://doi.org/10.1021/ef070025k

40. Abad A, Adánez J, Cuadrat A, García-Labiano F, Gayán P, de Diego LF. Kinetics of redox reactions of ilmenite for chemical-looping combustion. Chemical Engineering Science. 2011;66(4):689-702. https://doi.org/10.1016/j.ces.2010.11.010

41. Velasco-Sarria FJ, Forero CR, Adánez-Rubio I, Abad A, Adánez J. Assessment of low-cost oxygen carrier in South-western Colombia, and its use in the in-situ gasification chemical looping combustion technology. Fuel. 2018;218:417-24. https://doi.org/10.1016/j.fuel.2017.11.078

42. Linderholm C, Knutsson P, Schmitz M, Markström P, Lyngfelt A. Material balances of carbon, sulfur, nitrogen and ilmenite in a 100 kW CLC reactor system. Int J Greenhouse Gas Control. 2014;27:188. https://doi.org/10.1016/j.ijggc.2014.05.001

43. Carrillo A, Forero CR. Characterization for Disposal of the Residues Produced by Materials Used as Solid Oxygen Carriers in an Advanced Chemical Looping Combustion Process. Applied Sciences. 2018;8:1787. https://doi.org/10.3390/app8101787

44. Adánez J, Cuadrat A, Abad A, Gayán P, de Diego LF, García-Labiano F. Ilmenite activation during consecutive redox cycles in chemical-looping combustion. Energy and Fuels. 2010;24(2):1402-13. https://doi.org/10.1021/ef900856d

45. Abad A, Adánez J, García-Labiano F, de Diego LF, Gayán P. Modeling of the chemical-looping combustion of methane using a Cu-based oxygen-carrier. Combustion and Flame. 2010;157(3):602-15. https://doi.org/10.1016/j.combustflame.2009.10.010

46. Adanez J, Abad A, Garcia-Labiano F, Gayan P, de Diego LF. Progress in Chemical-Looping Combustion and Reforming technologies. Progress in Energy and Combustion Science. 2012;38(2):215-82. https://doi.org/10.1016/j.pecs.2011.09.001

doi: 10.25100/iyc.v27i1.14807

47. UPME. Sistema de información minero Colombiano - SIMCO: Unidad de Planeación Minero-energética; 2024 [Available from: https://www1.upme.gov.co/simco/Cifras-Sectoriales/Paginas/manganeso.aspx.

48. Cabello A, Mendiara T, Abad A, Adánez J. Techno-economic analysis of a chemical looping combustion process for biogas generated from livestock farming and agro-industrial waste. Energy Conversion and Management. 2022;267:115865. https://doi.org/10.1016/j.enconman.2022.115865

doi: 10.25100/iyc.v27i1.14807